Biosensors and Bioelectronics 41 (2013) 875–879

Contents lists available at SciVerse ScienceDirect

Biosensors and Bioelectronics

journal homepage: www.elsevier.com/locate/bios

Short communication

In-situ synthesis of fluorescent gold nanoclusters with electrospun fibrous membrane and application on Hg (II) sensing

Yuqing Cai [a], Lei Yan [a], Guangyue Liu [a], Hongyan Yuan [b,*], Dan Xiao [b,*]

[a] College of Chemistry, Sichuan University, No. 29 Wangjiang Road, Chengdu, PR China
[b] College of Chemical Engineering, Sichuan University, No. 29 Wangjiang Road, Chengdu, PR China

ARTICLE INFO

Article history:
Received 26 June 2012
Received in revised form
29 August 2012
Accepted 31 August 2012
Available online 7 September 2012

Keywords:
Gold nanoclusters
Electrospinning
In-situ
Mercury
Fluorescence

ABSTRACT

In the present study, a method for in-situ preparation of fluorescent gold nanoclusters with bovine serum albumin/poly(ethylene oxide) electrospun membrane (BSA/PEO-Au NCs) has been developed to detect Hg^{2+}. In this work, Au NCs were immobilized both inside and on the surface of fibrous membrane using one-step reduction of $HAuCl_4$ by BSA. The as-prepared BSA/PEO-Au NCs were able to emit intensive red fluorescence under the excitation of visible light, and the fluorescence could be quenched by Hg^{2+}. The results indicate that the as-prepared BSA/PEO-Au NCs exhibit good sensitivity towards Hg^{2+}, which might be benefit from the large specific surface area of BSA/PEO fibrous membrane. The biosensor exhibits a linear response to Hg^{2+} concentrations ranging from 0.5 nM to 75 nM with a limit of detection (LOD) of 57 pM. Moreover, BSA/PEO-Au NCs shows good selectivity towards other common metal ions. With the advantages of the simple preparation process and good detection performance, the proposed method is anticipated to fabricate other sensitive fluorescence fiber-based sensors of metal nanoclusters.

1. Introduction

Fluorescent gold nanoclusters have been developed extensively due to their good biocompatibility, ultra-small size and fluorescence property (Wilcoxon and Abrams, 2006). To date, fluorescent Au NCs have been created through several approaches successfully, such as using thiols (Jin, 2010; Negishi et al., 2004), polymers (Zheng et al., 2003; Huang et al., 2011), proteins etc. Proteins, such as BSA, have also been utilized as ideal agent during the formation of Au NCs. Xie and co-workers (2009, 2010) first reported fluorescent Au NCs synthesized with BSA and further application on Hg^{2+} ions sensing. Inspired by this finding, electrochemiluminescence (Li et al., 2011), CN^- sensor (Liu et al., 2010) and NO_x sensor (Yan et al., 2012) based on BSA-stablized Au NCs have been reported. Recently, researchers also found other proteins could be used to fabricate fluorescent Au NCs (Lin and Tseng, 2010; Wen et al., 2011; Xavier et al., 2010). It is worth noting that most of these Au NCs exist in the form of solution, here we develop a facile approach to in-situ synthesize fluorescent Au NCs with electrospun fibrous membrane, Au NCs could be in-situ prepared on the membrane and expected to fabricate into solid sensor such as test paper.

Electrospinning has been a wonderful technique for generating long fibers from various materials including polymers, composites and biomacromolecules (Greiner and Wendorff, 2007; Li and Xia, 2004). It provides ability to produce fibers with typical diameters from tens of nanometers to few micrometers. The surface area of electrospun fibrous membrane with porous structure is about one to two orders of magnitude higher than that of continuous thin film (Wang et al., 2002). The electrospun nanofibers which provide large amount of available surface area and porous structure have potential to provide extra high sensitivity in sensing applications (Liu et al., 2004; Wang et al., 2002).

In this paper, we present an effective route to in-situ synthesize fluorescent Au NCs with BSA/PEO electrospinning fibrous membrane and its application on Hg^{2+} sensing (Scheme 1). Both BSA and PEO have good biocompatibility so that BSA/PEO-Au NCs are expected to be "green" materials for further application (Gensheimer et al., 2007; Kowalczyk et al., 2008). To our knowledge, this is the first report on using electrospun fiber membrane to in-situ prepare Au NCs with red fluorescence. The water-solubility of BSA/PEO nanofibers changed after aging was found since the degeneration of BSA. Optimum conditions for fabricating BSA/PEO-Au NCs were investigated in detail. We have demonstrated that as-prepared BSA/PEO-Au NCs could be applied to Hg^{2+} detection,

* Corresponding authors. Tel.: +86 28 85415029; fax: +86 28 85416029.
E-mail addresses: yuan_hy@scu.edu.cn (H. Yuan), xiaodan@scu.edu.cn (D. Xiao).

0956-5663/$ - see front matter © 2012 Elsevier B.V. All rights reserved.
http://dx.doi.org/10.1016/j.bios.2012.08.064

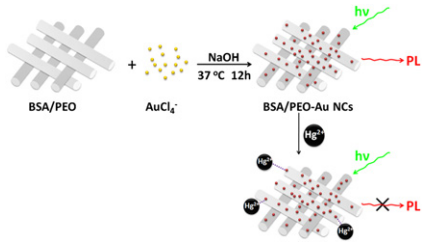

Scheme 1. Schematic of the synthesis of fluorescent gold nanoclusters with electrospun fibrous membrane and quenched by Hg^{2+}.

and it exhibit high sensitivity and excellent selectivity to Hg^{2+} with a limit of detection down to 57 pM.

2. Experiment

2.1. Chemical and materials

Lyophilized BSA was purchased from Shanghai Bio Life Science & Technology Co., Ltd. (Shanghai, China). PEO with an average molecular weight of 9,00,000 and hydrogen tetrachloroaurate (III) trihydrate ($HAuCl_4 \cdot 3H_2O$) were obtained from Aldrich (Milwaukee, WI, USA). All reagents were of analytical grade and used as received without further purification.

2.2. Apparatus

Optical microscopy measurements were captured on a M-LCD (View Solutions Inc., Beijing, China). SEM measurements were made on a S-4800 filed emission scanning electronic microscope (FESEM) (Hitachi, Tokyo, Japan) at an accelerating voltage of 5 kV. Fluorescence measurements were performed on F-7000 fluorescence spectrophotometer (Hitachi, Tokyo, Japan). The TEM and HRTEM images were obtained by an FEI Tecnai F-20 field-emission HRTEM (Hills-boro, OR, USA) operating at 200 kV. Infrared spectra were acquired on a Thermo Nicolet 6700 infrared spectrophotometer (Vernon Hills, Illinois, USA). X-ray photoelectron spectroscopy (XPS) was conducted on a Kratos XSAM 800 photoelectron spectrometer (Manchester, UK). Confocal microscopy images were obtained on Leica TCS SP5 confocal microscope (Germany). The electrospinning apparatus consisted of a high-voltage power supply (DW-P303-1ACCC, Dongwen High Voltage Inc., Tianjin, China), a syringe pump, a syringe, a stainless steel needle (d=0.55 mm) and a grounded collector (aluminium foil).

2.3. Preparation of BSA/PEO nanofiber membrane

BSA/PEO nanofibers were prepared by electrospinning using PEO to increase the viscosity of precursor solution (Kowalczyk et al., 2008). Typically, 80 mg BSA and 40 mg PEO powder were dissolved in 1.0 mL H_2O with magnetically stirring at room temperature for 1 h to obtain a homogeneous solution for electrospinning. The needle was connected to the high-voltage supply with applied voltage of 16 kV. The spinning distance between the tip of the needle and the collector was set at 25 cm. The flow-rate for the precursor solution was controlled using a syringe pump with 0.2 mL/h. After the electrospun fibrous membrane was formed, it was gently removed from the Al foil and aged in oven at 80 °C for 60 h. All electrospinning experiments were carried out at 21 °C and a relative humidity of 40%.

2.4. In-situ synthesis of Au NCs with BSA/PEO fibrous membrane

All glasswares were washed with Aqua Regia (HCl: HNO_3 volume ratio=3: 1) and rinsed with doubly distilled water. In a typical experiment, BSA/PEO fibrous membrane (5.0 mg) was added into $HAuCl_4$ solution (1980 μL, 3.0 mM). NaOH solution (120 μL, 1.0 M) was introduced 2 min later, and the reaction was allowed to proceed at 37 °C for 12 h. The as-synthesized BSA/PEO-Au NCs were washed through distilled water.

3. Result and discussion

3.1. Synthesis and characterization of BSA/PEO-Au NCs

Under the optimal electrospun conditions (Fig. S1), the BSA/PEO electrospun nanofibers are almost uniform with average diameter of 215 nm (Fig. S2a). Both BSA and PEO are water soluble compounds, BSA/PEO fibers could not be used for in-situ fabricating Au NCs when the reaction takes place in aqueous solution. However, heating processing would lead to degeneration of protein when the temperature is higher than critical temperature and change the water solubility of protein (Mishina and Kojima, 2008). BSA/PEO nanofibers were aged at 80 °C for 60 h in order to obtain insoluble fibers to in-situ fabricate Au NCs. After aging, equivalent BSA/PEO nanofibers before and after aging were immersed into water, the intrinsic fluorescence of tryptophan residues derived from BSA in solution was only 1% of original fluorescence intensity before (Figs. S3 and S4), inferring water solubility of BSA/PEO fibers has changed. Fig. S5 shows the FT-IR second-derivation spectra, the band from native structure (1629 cm^{-1}) decreased while the peak from turns (1664 cm^{-1}) increased, which suggest the change of the structure of BSA after aging (Zhang and Yan, 2005). Contrasting to the fibers without aging, the average diameter of aging BSA/PEO slightly decreased to 207 nm and a little cementation among nanofibers for aging BSA/PEO could be observed in Fig. S2b. However, it did not affect the general morphology of BSA/PEO nanofibers.

The optimal condition with 2.83 mM $HAuCl_4$ and 57.1 mM NaOH for producing the highest fluorescence intensity of BSA/PEO-Au NCs complexes was also obtained (Fig. S6a). The BSA/PEO-Au NCs membrane remained fibrous and the average diameter of fibers increased to 384 nm through in-situ fabrication of Au NCs (Fig. S2c), this change might be ascribed to swelling of fibers caused by dipping into alkaline solution for a long time. As shown in Fig. 1a, Au NCs with uniform size are well dispersed on nanofibers with average diameter of *ca.* 5 nm which is consistent with the report (Yan et al., 2012). The inset in the Fig. 1a suggests the lattice fringes of Au NCs are consistent with metallic gold having a discerned lattice spacing of 2.3 Å, which corresponds to the d spacing of the {111} crystal plane of Au (Buffat et al., 1991). The selected area electron diffraction (SAED) pattern indicates the presence of the well organized Au nanocrystals in BSA/PEO-Au NCs. Fig. 1b shows the cross-sectional TEM of BSA/PEO-Au NCs, it clearly reveals the existence of Au NCs in the both inside and surface of BSA/PEO-Au NCs fibers.

The as-prepared BSA/PEO-Au NCs exhibited a wide excitation band from 350 nm to 600 nm, and the emission band ranged between 550 nm and 700 nm centered at 625 nm (Fig. S7a). We chose 495 nm which was in visible range as excitation wavelength to avoid interference of biological intrinsic fluorescence in further applications. The color of as-prepared membrane changed from white to light brown and emitted intensive red fluorescence under the UV lamp (365 nm) (inset of Fig. S7a). It was observed that the BSA/PEO-Au NCs exhibiting red fluorescence *via* the confocal microscope (Fig. 1c), which is in agreement with the

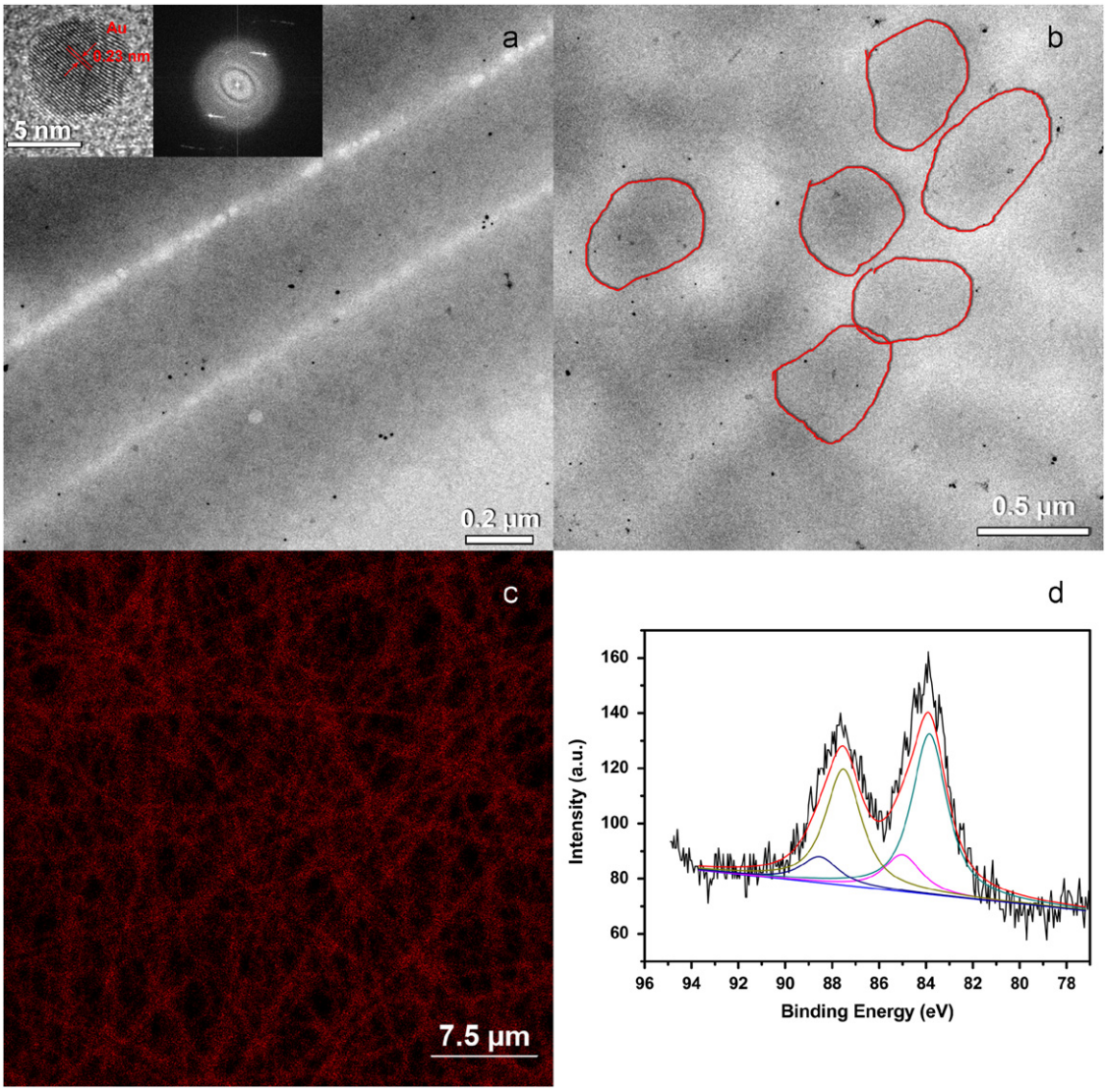

Fig. 1. (a) TEM image of BSA/PEO-Au NCs. The left and right insets display the HRTEM image and SAED pattern of Au NCs, respectively. (b) Cross-sectional TEM image of BSA/PEO-Au NCs. (c) Fluorescence images of BSA/PEO-Au NCs fibrous membrane. (d) XPS spectra of Au 4f core-level for BSA/PEO-Au NCs.

fluorescence spectrum of BSA/PEO-Au NCs. The XPS spectra show that the Au $4f_{7/2}$ spectrum could be deconvoluted into two distinct components centered at binding energies of 83.9 and 85.0 eV (Fig. 1d), which could be assigned to Au(0) and Au(I), respectively (Xie et al., 2009). In general, fluorescent Au NCs were synthesized using BSA/PEO electrospun fibrous membrane successfully.

3.2. *Fluorescent sensing of Hg (II)*

In the previous studies of BSA-Au NCs, the Hg^{2+} quenched the fluorescence of BSA-Au NCs in solution attributing to high specificity between Hg^{2+} and Au^{+} (Xie et al., 2010). BSA/PEO-Au NCs was supposed to fluorescent sensing of Hg^{2+} effectively. It was found that BSA/PEO-Au NCs exhibited ultra sensitive characteristics for the detection of Hg^{2+} by quenching fluorescence of BSA/PEO-Au NCs (Fig. 2a). When the BSA/PEO-Au NCs fibrous membrane was immersed in Hg^{2+} solution, the fluorescent emission under UV lamp illumination turned to weaker which could be observed with naked eye (Fig. S8). As the concentration of Hg^{2+} increased, fluorescence intensity of BSA/PEO-Au NCs decreased gradually (Fig. 2a). As shown in the inset of Fig. 2a, the response of the sensor coincides with modified Stern–Volmer equation (Liu et al., 1998; Zhang et al., 2002), there is a linear correlation between expression log $[(I_0-I)/I]$ and the logarithm of concentration of Hg^{2+} over the range of 0.5–75 nM with a linear related coefficient of $R^2=0.992$. Here I_0 is the original fluorescence intensity of BSA/PEO-Au NCs in water, I is the fluorescence intensity of BSA/PEO-Au NCs in different concentration of Hg^{2+}, and c is the concentration of Hg^{2+} (M). The relative standard deviation was 3.5% for three repeated measurements of 7.5 nM Hg^{2+}. The LOD of the biosensor is estimated to 57 pM at an signal-to-noise ratio of 3 for Hg^{2+}, which is much lower than the highest concentration (10 nM) of mercury in drinking water permitted by United States Environmental Protection Agency (EPA).

To investigate whether our system is specific for Hg^{2+}, we measured the fluorescence response of BSA/PEO-Au NCs with Hg^{2+} and several common cations with the concentration of interference was 40-fold over Hg^{2+}. As shown in Fig. 2b, only Hg^{2+} could cause a drastic decrease in the fluorescence intensity. The highly specificity of Hg and BSA-Au NCs provided excellent selectivity of BSA/PEO-Au NCs to determination Hg^{2+} (Hu et al.,

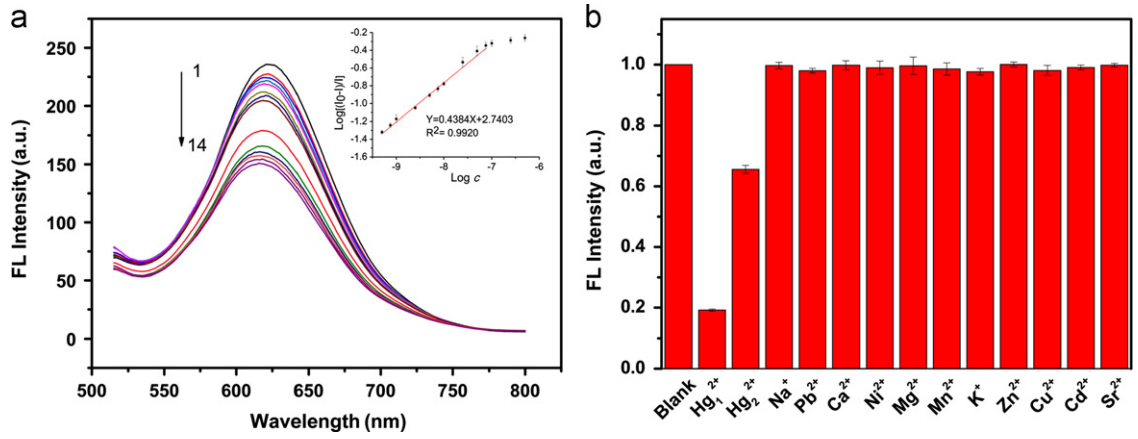

Fig. 2. (a) The fluorescence response of BSA/PEO-Au NCs upon addition of various concentrations of Hg^{2+} (from top: 1: 0, 2: 0.5, 3: 0.75, 4: 1.0, 5: 2.5, 6: 5.0, 7: 7.5, 8: 10, 9: 25, 10: 50,11: 75, 12: 100, 13: 250, 14: 500 nM). Inset: Plot of $\log[(I_0-I)/I]$ of BSA/PEO-Au NCs verses the log concentration of Hg^{2+}. (b) Selectivity of BSA/PEO-Au NCs sensor for Hg^{2+} over other cations: the concentration of Hg_1^{2+} and Hg_2^{2+} were 10 μM and 250 nM, respectively. The interference cations at the concetration of 10 μM.

2010; Xie et al., 2010). The above results indicated that BSA/PEO-Au NCs was highly selective towards Hg^{2+} over other cations.

In comparison with other fluorescence methods shown in Table S1, the proposed method exhibits the most sensitive to detect Hg^{2+}. The ultrasensitive response of BSA/PEO-Au NCs for Hg^{2+} might result from the relatively huge specific surface area of electrospun membrane, which allows the access of analytes to reactive sites of BSA/PEO-Au NCs with minimal resistance (Ding et al., 2010). With the increasing concentration of Hg^{2+}, the maximum emission wavelength was blue-shift slightly, which indicated the change of surface state of BSA/PEO-Au NCs due to the Hg^{2+} bound onto its surface during the reaction (Hu et al., 2010). On the basis of previous studies, the Hg^{2+} induced fluorescence quenching of the BSA-Au NCs is probably attributed to the formation of metallophilic bonding between Hg^{2+} ($4f^{14}5d^{10}$) and Au^{+} ($4f^{14}5d^{10}$) (Xie et al., 2010). The dispersion forces between closed-shell metal atoms are highly specific and strong, which are greatly magnified by relativistic effects involve heavy ions such as Hg^{2+} and Au^{+}. The proposed sensing mechanism was further supported by the XPS data. As shown in Fig.1d, the XPS data indicates that the small amount of Au(I) (about 19%) present on the surface of the Au core, which should have strong and specific interactions with Hg^{2+}. The high specificity of Hg^{2+}–Au^{+} interactions provided the excellent selectivity of BSA/PEO-Au NCs towards detecting Hg^{2+} over other metal ions. Thus, we attributed the high sensitivity and selectivity to the relatively huge specific surface area and $5d^{10}$ (Hg^{2+})–$5d^{10}$ (Au^{+}) metallophilic interaction, which was consistent with previous reports.

4. Conclusions

We have presented an effective route to in-situ synthesize Au NCs with red fluorescence using BSA/PEO fibrous membrane and its application on Hg (II) sensing. The as-prepared BSA/PEO-Au NCs could be excited by visible light (495 nm) to avoid intrinsic fluorescence of biological system. According to our knowledge, it is an example to prepare fluorescent Au NCs combined with electrospinning technology. Our method shows a linear response to Hg (II) concentrations ranging from 0.5 nM to 75 nM with a linear coefficient of $R^2=0.992$. And the detection limit of the biosensor is estimated to 57 pM. The BSA/PEO-Au NCs biosensor shows better sensitivity than most fluorescence methods reported, and there is no obvious interference over other metal ions. This method involved electrospinning technology is expected to extend to other proteins and metal nanoclusters to in-situ fabrication of sensitive fluorescence materials.

Acknowledgment

This work was supported by the National Natural Science Foundation of China (20927007 and 21075083). We express our thanks to Ms Shanling Wang and Ms Guiping Yuan of the Analytical and Testing Center of Sichuan University for taking the TEM and HRTEM images.

Appendix A. Supporting information

Supplementary data associated with this article can be found in the online version at http://dx.doi.org/10.1016/j.bios.2012.08.064.

References

Buffat, P.A., Flueli, M., Spycher, R., Stadelmann, P., Borel, J.P., 1991. Faraday Discussions 92, 173–187.
Ding, B., Wang, M.R., Wang, X.F., Yu, J.Y., Sun, G., 2010. Materials Today 13, 16–27.
Gensheimer, M., Becker, M., Brandis-Heep, A., Wendorff, J.H., Thauer, R.K., Greiner, A., 2007. Advanced Materials 19, 2480–2482.
Greiner, A., Wendorff, J.H., 2007. Angewandte Chemie-International Edition 46, 5670–5703.
Hu, D.H., Sheng, Z.H., Gong, P., Zhang, P.F., Cai, L.T., 2010. Analyst 135, 1411–1416.
Huang, X., Luo, Y., Li, Z., Li, B.Y., Zhang, H., Li, L., Majeed, I., Zou, P., Tan, B.E., 2011. Journal of Physical Chemistry C 115, 16753–16763.
Jin, R.C., 2010. Nanoscale 2, 343–362.
Kowalczyk, T., Nowicka, A., Elbaum, D., Kowalewski, T.A., 2008. Biomacromolecules 9, 2087–2090.
Li, D., Xia, Y.N., 2004. Advanced Materials 16, 1151–1170.
Li, L.L., Liu, H.Y., Shen, Y.Y., Zhang, J.R., Zhu, J.J., 2011. Analytical Chemistry 83, 661–665.
Lin, Y.H., Tseng, W.L., 2010. Analytical Chemistry 82, 9194–9200.
Liu, H.Q., Kameoka, J., Czaplewski, D.A., Craighead, H.G., 2004. Nano Letters 4, 671–675.
Liu, W.H., Wang, Y., Tang, J.H., Shen, G.L., Yu, R.Q., 1998. Talanta 46, 679–688.
Liu, Y.L., Ai, K.L., Cheng, X.L., Huo, L.H., Lu, L.H., 2010. Advanced Functional Materials 20, 951–956.
Mishina, H., Kojima, M., 2008. Wear 265, 655–663.
Negishi, Y., Takasugi, Y., Sato, S., Yao, H., Kimura, K., Tsukuda, T., 2004. Journal of the American Chemical Society 126, 6518–6519.
Wang, X.Y., Drew, C., Lee, S.H., Senecal, K.J., Kumar, J., Sarnuelson, L.A., 2002. Nano Letters 2, 1273–1275.
Wen, F., Dong, Y.H., Feng, L., Wang, S., Zhang, S.C., Zhang, X.R., 2011. Analytical Chemistry 83, 1193–1196.
Wilcoxon, J.P., Abrams, B.L., 2006. Chemical Society Reviews 35, 1162–1194.

Xavier, P.L., Chaudhari, K., Verma, P.K., Pal, S.K., Pradeep, T., 2010. Nanoscale 2, 2769–2776.
Xie, J.P., Zheng, Y.G., Ying, J.Y., 2009. Journal of the American Chemical Society 131, 888–889.
Xie, J.P., Zheng, Y.G., Ying, J.Y., 2010. Chemical Communications 46, 961–963.
Yan, L., Cai, Y.Q., Zheng, B.Z., Yuan, H.Y., Guo, Y., Xiao, D., Choi, M.M.F., 2012. Journal of Materials Chemistry 22, 1000–1005.
Zhang, J., Yan, Y.B., 2005. Analytical Biochemistry 340, 89–98.
Zhang, X.B., Guo, C.C., Li, Z.Z., Shen, G.L., Yu, R.Q., 2002. Analytical Chemistry 74, 821–825.
Zheng, J., Petty, J.T., Dickson, R.M., 2003. Journal of the American Chemical Society 125, 7780–7781.